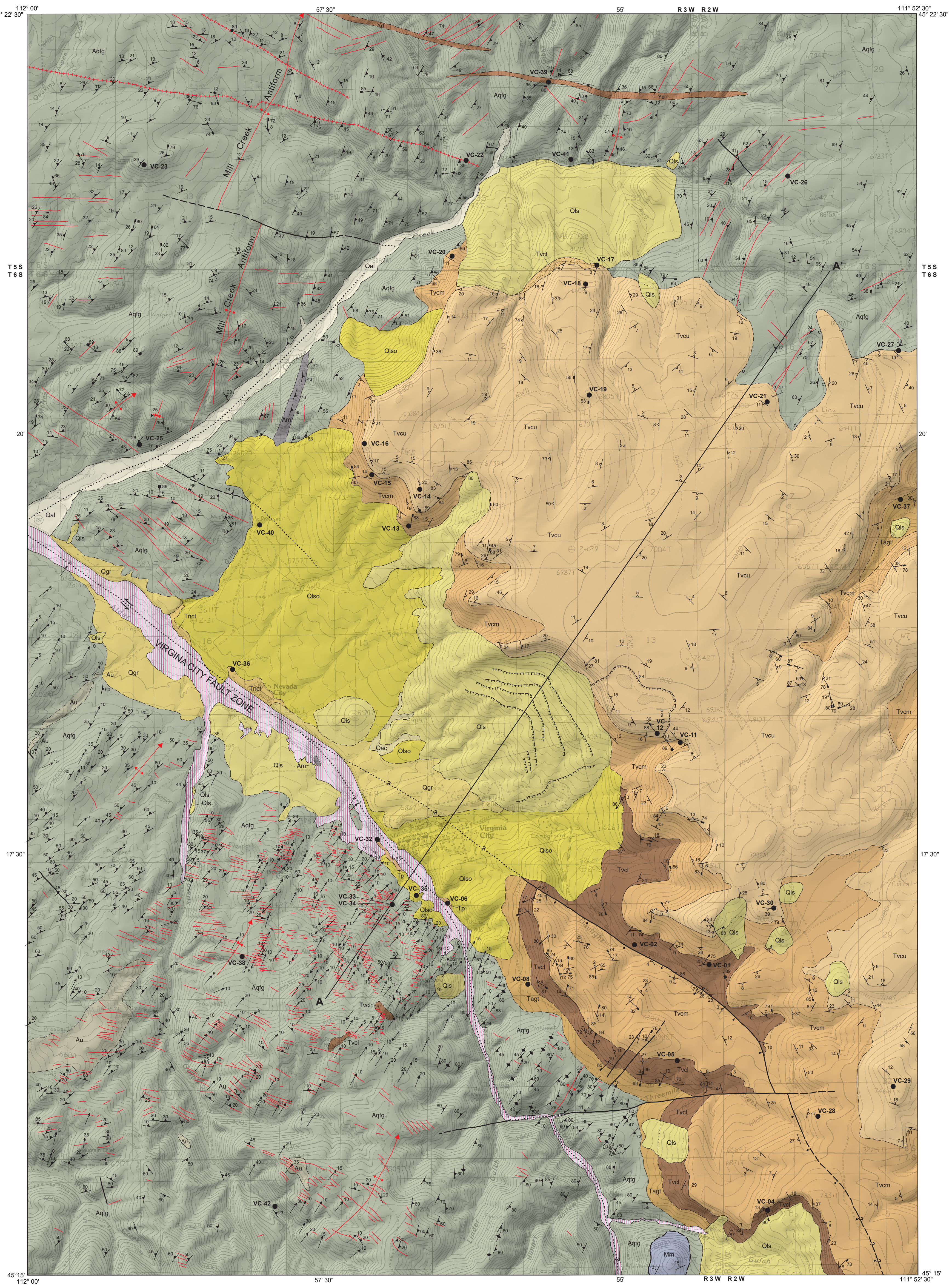

Base map produced by the United States Geological Survey
Virginia City 1:24,000-scale quadrangle map
Control by: USGS and NOS/NOAA
Compiled from aerial photographs taken 1982
Field checked: 1985 Map edited: 1988
Projection: Lambert Conformal Conic
Grid:1000 meter Universal Transverse Mercator Zone 12
UTM grid declination: 0°40' West
1988 Magnetic North Declination: 16° East
Vertical Datum: National Geodetic Vertical Datum of 1929
Horizontal Datum: 1927 North American Datum

Shaded relief created from 10 meter digital elevation
model from U.S. Geological Survey National Elevation Dataset.

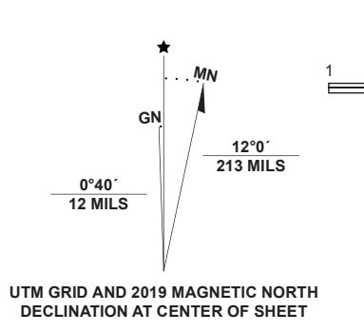

SCALE 1:24,000

CONTOUR INTERVAL 40 FEET
NATIONAL GEODETIC VERTICAL DATUM OF 1929

Maps may be obtained from:
Publications Office
Montana Bureau of Mines and Geology
1300 West Park Street
Butte, Montana 59701-8997
Phone: (406) 496-4167 Fax: (406) 496-4451
http://www.mbmg.mtech.edu

Cross Section A–A'

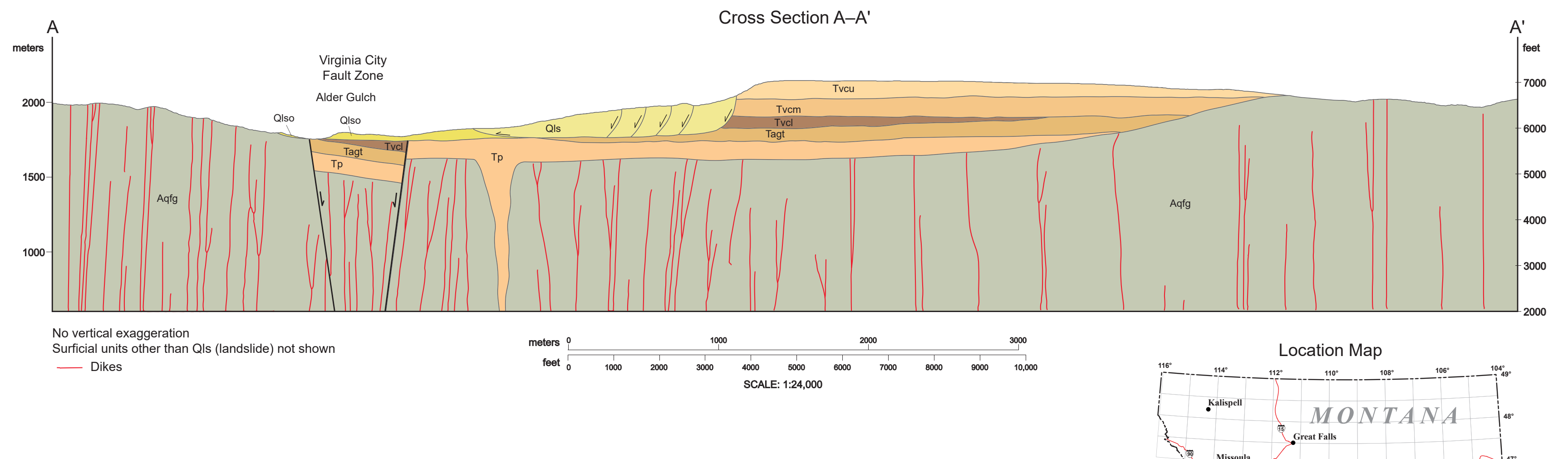

No vertical exaggeration
Surficial units other than Qls (landslide) not shown
— Dikes

Location Map

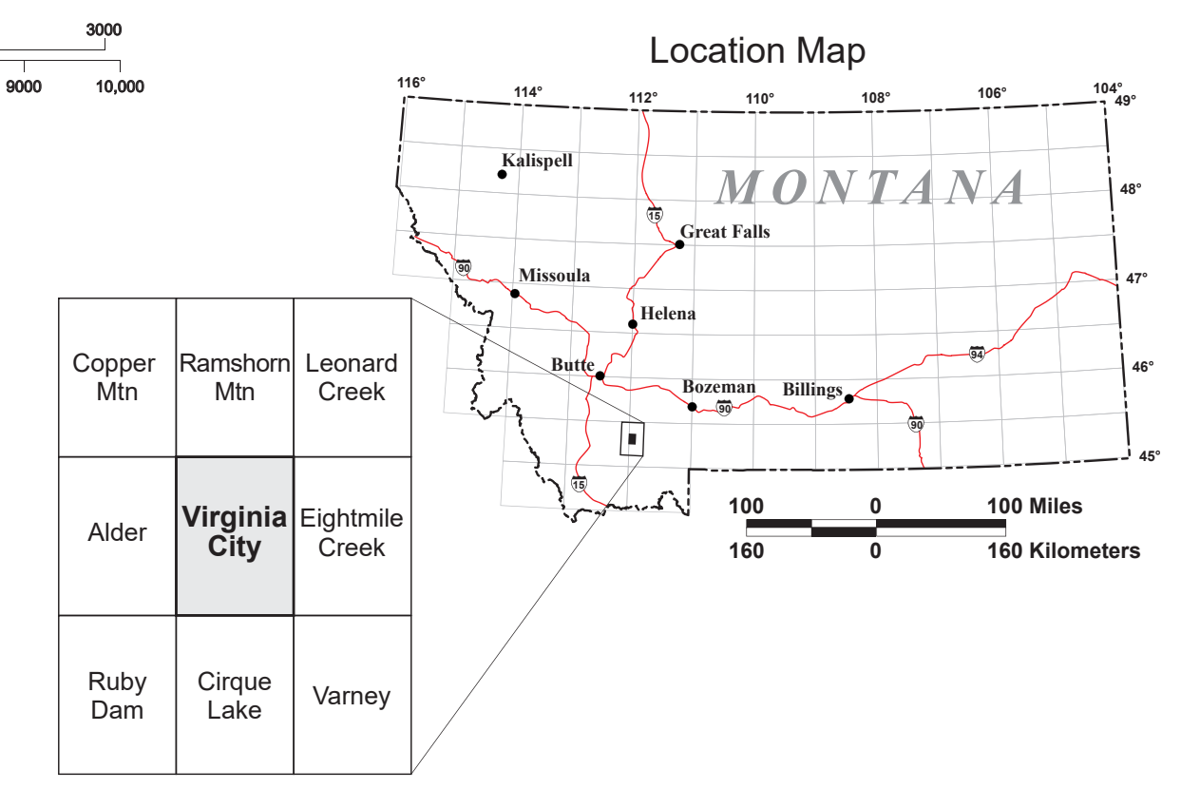

Research supported by the U.S. Geological Survey, National Cooperative Geologic Mapping Program, under USGS award G17AC00257.
GIS production: Yiwen Li, Christopher Smith, and Paul Thale, MBMG. Map layout: Susan Smith, MBMG. Editing: Susan Barth, MBMG.

CORRELATION CHART

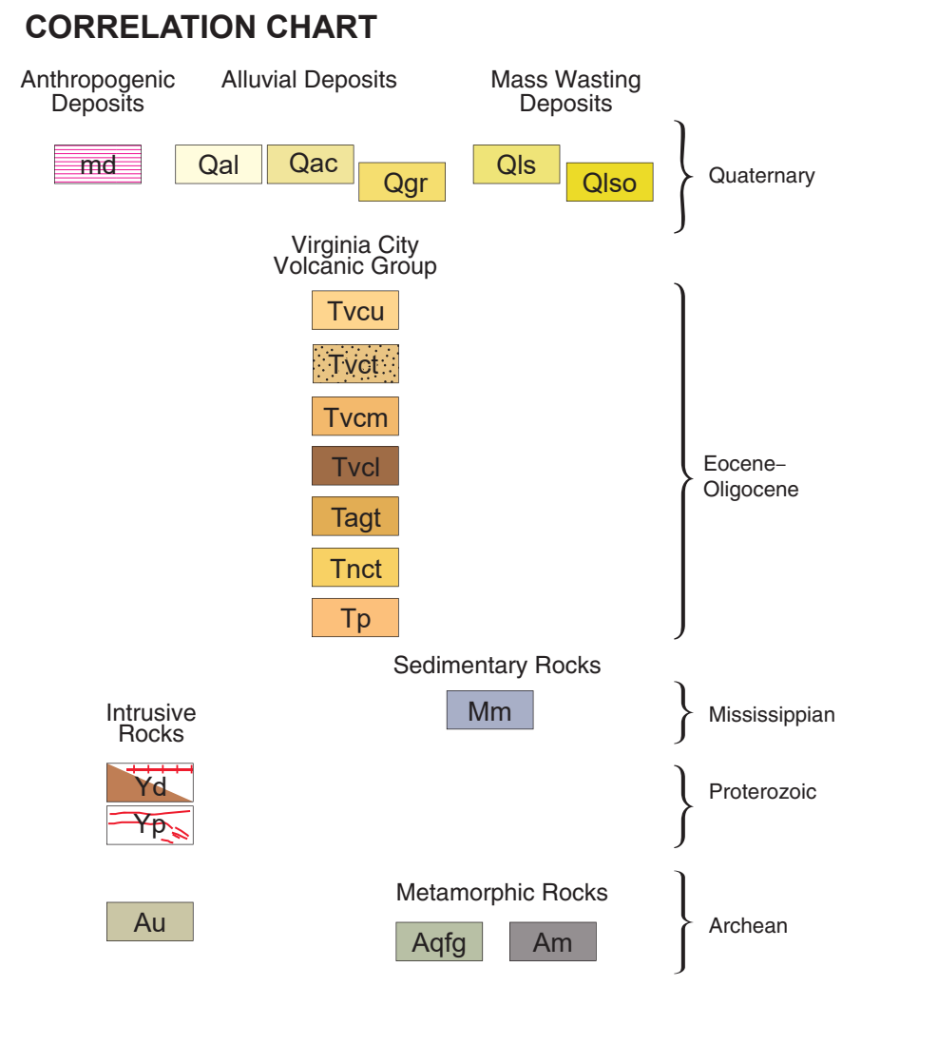

MAP SYMBOLS

- Contact: dashed where approximately located; queried where unknown
- Normal fault: dashed where approximately located, dotted where concealed, bar and ball on downthrown side; queried where unknown
- High-angle fault: dashed where approximately located; dotted where concealed; arrows show lateral motion where discernable; queried where unknown
- Synform: showing trace of axial plane and plunge direction where known
- Antiform: showing trace of axial plane and plunge direction where known
- Internal or minor scarp in landslide. Hachures point down scarp
- Diabase dike (Yd)
- Pegmatite dike (Yp)
- 38 Strike and dip of inclined beds
- 85 Strike and dip of cleavage
- 28 Strike and dip of metamorphic foliation
- Vertical metamorphic foliation
- 10 Trend and plunge direction of metamorphic lineation, commonly a mineral lineation
- 40 Strike and dip of igneous foliation
- 87 or 87 Strike and dip of inclined joint
- Vertical or near-vertical joint
- VC-25 Specimen location with sample number

Table 1. Major and trace element chemistry.

Sample ID	VC-01	VC-02	VC-04	VC-05	VC-06	VC-08	VC-11	VC-12	VC-13	VC-14	VC-15	VC-16
Map unit	Tvcl	Tvcl	Tvcl	Tvcl	Tp	Tagt	Tvcm	Tvcu	Tvcm	Tvcu	Tvcm	Tvcu
Lithology	Ba lava	Ba TAnd lava	Ba lava	Ba lava	Da porphyry	Tuff	Ba TAnd lava	Ba TAnd lava	Ba lava	TAnd lava	TBa lava	Ba TAnd lava
Latitude (°N)	45.2807	45.2827	45.2564	45.2712	45.2868	45.2788	45.3028	45.3036	45.3242	45.3278	45.3293	45.3324
Longitude (°W)	111.9051	111.9156	111.8969	111.9096	111.9418	111.9305	111.9091	111.9124	111.9473	111.9457	111.9525	111.9535
Major elements (wt%)												
SiO_2	47.36	50.23	49.21	46.94	65.12	32.43	52.22	51.31	47.53	57.56	48.82	54.57
TiO_2	1.40	1.50	1.50	1.39	0.56	0.34	1.34	1.43	1.62	1.04	1.60	1.13
Al_2O_3	15.64	15.52	15.79	15.50	15.77	7.16	17.61	15.99	16.75	15.65	17.25	15.93
FeO*	9.13	9.28	8.71	9.13	3.90	2.34	8.80	8.19	9.22	6.37	9.42	6.90
MnO	0.16	0.14	0.16	0.16	0.02	0.25	0.14	0.14	0.16	0.12	0.15	0.13
MgO	9.94	7.13	7.82	9.96	0.77	0.97	3.21	6.57	7.41	4.95	4.69	5.66
CaO	9.51	7.19	8.74	8.96	3.10	27.34	7.60	7.26	9.82	6.37	8.93	7.72
Na_2O	2.98	3.37	3.06	2.53	4.01	0.83	3.81	3.55	3.24	3.60	3.60	3.56
K_2O	0.99	1.79	1.71	1.33	2.56	1.68	2.14	2.22	1.10	2.60	1.64	2.32
P_2O_5	0.33	0.49	0.36	0.32	0.19	0.16	0.35	0.41	0.39	0.27	0.39	0.30
Sum	97.43	96.65	97.06	96.23	95.99	73.52	97.21	97.07	97.24	98.52	96.49	98.22
LOI	2.19	2.69	1.94	3.01	3.42	25.72	2.42	2.14	2.10	0.86	3.11	1.17
Trace elements (ppm)												
Ni+	202.28	140.00	128.10	192.80	23.30	5.25	37.91	102.49	105.17	98.40	45.27	100.39
Cr+	324.07	172.83	240.60	313.60	44.10	11.92	27.56	148.26	195.62	172.60	36.52	181.80
V+	199.40	141.89	190.10	197.70	76.80	39.90	177.91	147.06	198.01	121.80	177.91	138.37
Ga+	15.02	16.42	15.90	15.70	19.60	9.80	17.91	16.22	17.01	17.20	17.31	16.67
Cu+	45.87	37.91	39.50	39.60	9.80	17.57	29.15	26.67	52.64	27.80	32.24	25.96
Zn+	74.72	82.68	79.20	81.10	68.80	56.96	79.00	72.34	83.68	68.80	80.40	77.67
La	25.41	44.66	36.43	26.02	52.55	26.70	38.49	43.55	28.48	44.83	32.93	40.53
Ce	50.21	83.63	68.60	51.19	88.34	42.82	71.47	80.20	56.85	79.13	62.53	73.84
Pr	6.11	9.60	8.04	6.21	9.94	5.51	8.08	9.03	7.01	8.54	7.48	8.25
Nd	24.29	35.76	30.33	24.44	34.64	20.54	30.33	33.27	27.92	30.39	28.48	29.64
Sm	5.12	6.61	5.97	5.05	5.33	4.18	5.76	6.14	5.74	5.49	5.78	5.47
Eu	1.65	2.04	1.86	1.64	1.43	0.91	1.81	1.89	1.88	1.52	1.84	1.63
Gd	4.72	5.93	5.47	4.81	3.57	4.04	5.24	5.47	5.44	4.74	5.42	4.80
Tb	0.77	0.91	0.88	0.77	0.46	0.67	0.84	0.84	0.86	0.73	0.88	0.75
Dy	4.58	5.25	5.13	4.53	2.33	4.15	5.02	5.10	5.17	4.23	5.22	4.42
Ho	0.93	1.03	1.04	0.92	0.42	0.89	1.01	1.02	1.03	0.85	1.06	0.90
Er	2.43	2.73	2.73	2.41	1.01	2.49	2.70	2.71	2.69	2.30	2.75	2.37
Tm	0.35	0.38	0.39	0.35	0.14	0.39	0.38	0.39	0.37	0.33	0.40	0.33
Yb	2.17	2.36	2.39	2.12	0.84	2.48	2.38	2.47	2.33	2.09	2.37	2.14
Lu	0.32	0.37	0.38	0.33	0.13	0.39	0.38	0.37	0.36	0.34	0.38	0.34
Ba	780.29	1,051.91	976.08	783.53	1,734.43	793.82	1,214.81	1,235.66	867.04	1,324.10	954.72	1,243.21
Th	2.87	5.78	4.86	3.06	8.66	7.24	5.84	6.94	2.93	8.62	4.10	7.15
Nb	31.30	38.55	35.80	31.20	11.27	8.01	29.89	38.64	35.27	29.78	33.39	31.73
Y	22.72	25.93	25.65	22.59	10.75	26.12	25.38	26.00	25.35	22.31	26.47	22.68
Hf	2.98	4.40	4.00	2.98	4.14	2.78	4.33	4.35	3.62	4.39	3.90	4.13
Ta	1.88	2.34	2.18	1.88	0.66	0.62	1.79	2.32	2.02	1.91	1.93	1.99
U	0.78	1.50	1.22	0.81	1.37	2.68	1.44	1.85	0.81	1.83	1.03	1.59
Pb	3.83	9.47	8.67	4.90	27.41	15.08	8.10	10.47	6.30	14.17	5.30	15.60
Rb	25.52	40.98	40.24	31.52	48.05	59.96	51.11	52.14	35.12	52.62	36.58	43.77
Cs	0.88	1.79	0.55	1.39	1.52	2.71	0.87	0.96	1.57	0.78	0.45	0.50
Sr	549.21	526.95	524.18	513.65	806.46	184.98	530.67	589.89	645.27	487.31	558.83	538.32
Sc	27.46	19.59	25.12	26.82	7.17	7.71	20.93	20.61	27.41	17.04	23.01	18.99
Zr	121.48	182.78	164.29	122.55	156.14	105.26	175.36	179.39	153.68	179.52	165.80	169.75

Sample ID	VC-17	VC-18	VC-19	VC-20	VC-21	VC-22	VC-23	VC-25	VC-26	VC-27	VC-28	VC-29
Map unit	Tvct	Tvcu	Tvcu	Tvcm	Tvcu	Yd	Aqfg	Aqfg	Yp	Tvcu	Tvcm	Tvcu
Lithology	Tuff	TAnd lava	And lava	TAnd lava	TAnd lava	Diabase	Gneiss	Gneiss	Pegmatite	Ba lava	Ba lava	Ba TAnd lava
Latitude (°N)	45.3501	45.3482	45.3372	45.3509	45.3365	45.3604	45.3600	45.3323	45.3589	45.3415	45.2657	45.2686
Longitude (°W)	111.9208	111.9224	111.9219	111.9412	111.8969	111.9392	111.9845	111.9851	111.8940	111.8784	111.8898	111.8793
Major elements (wt%)												
SiO_2	40.52	56.96	56.95	61.06	55.75	49.39	70.43	70.11	75.83	48.26	49.25	50.01
TiO_2	0.49	1.08	1.06	0.90	1.12	1.21	0.64	0.68	0.01	1.49	1.44	1.59
Al_2O_3	9.83	15.83	15.59	15.15	15.82	13.75	12.12	12.85	14.89	16.54	15.64	17.21
FeO*	3.48	6.51	7.08	4.92	6.62	11.74	6.18	5.35	0.27	9.69	8.88	8.87
MnO	0.05	0.12	0.12	0.08	0.12	0.20	0.10	0.07	0.02	0.16	0.16	0.14
MgO	2.00	5.12	4.87	3.50	5.23	7.41	0.29	0.33	0.04	6.16	8.63	5.28
CaO	18.67	6.49	6.77	4.56	6.98	10.69	2.18	2.21	1.34	10.22	8.78	7.49
Na_2O	0.99	3.57	3.40	3.53	3.58	2.17	2.82	2.80	6.19	3.23	2.94	3.73
K_2O	1.49	2.60	2.39	3.37	2.43	1.40	4.13	4.73	0.65	1.19	1.66	2.12
P_2O_5	0.13	0.28	0.24	0.33	0.28	0.09	0.14	0.17	0.01	0.30	0.34	0.47
Sum	77.64	98.56	98.46	97.39	97.93	98.04	99.04	99.31	99.26	97.25	97.72	96.92
LOI	21.83	0.65	0.89	1.64	1.18	1.47	0.12	0.20	0.51	2.00	1.92	2.28
Trace elements (ppm)												
Ni+	18.58	98.80	90.20	75.12	98.31	88.80	5.77	4.60	5.07	72.83	155.62	52.54
Cr+	40.70	166.86	223.00	189.95	172.43	220.30	4.68	2.10	11.64	121.59	292.23	61.69
V+	52.22	131.84	126.70	89.25	144.47	318.50	11.24	8.70	2.99	183.58	186.46	160.29
Ga+	11.62	16.52	18.30	19.60	17.41	16.50	19.60	19.30	26.37	17.81	16.12	15.92
Cu+	20.71	29.35	39.10	25.47	29.75	151.00	10.65	9.60	3.48	50.75	42.79	26.77
Zn+	64.03	66.86	71.80	85.57	74.23	90.90	122.88	86.90	5.07	90.35	80.20	74.23
La	34.46	43.87	41.07	71.29	43.17	6.20	63.23	74.17	7.76	24.11	33.25	42.29
Ce	51.23	77.95	72.23	120.68	77.24	14.75	131.90	144.00	12.02	46.87	62.89	78.47
Pr	7.16	8.54	7.84	12.60	8.55	2.10	14.59	17.16	1.74	5.66	7.37	9.00
Nd	26.44	30.50	27.88	43.05	30.30	9.72	56.25	66.88	7.40	22.76	27.88	33.56
Sm	5.43	5.45	5.07	6.77	5.59	2.91	13.01	15.36	3.63	4.83	5.62	6.45
Eu	1.09	1.58	1.47	1.77	1.61	1.07	3.03	2.79	0.37	1.61	1.72	2.05
Gd	4.98	4.78	4.47	4.54	4.85	3.61	13.31	15.35	6.97	4.92	5.13	5.69
Tb	0.79	0.73	0.70	0.58	0.75	0.64	2.30	2.60	1.60	0.78	0.81	0.90
Dy	4.94	4.48	4.32	2.91	4.39	4.12	14.91	15.78	11.43	4.75	4.90	5.34
Ho	1.00	0.87	0.84	0.52	0.89	0.88	3.15	3.15	2.49	0.98	0.99	1.10
Er	2.78	2.31	2.27	1.22	2.36	2.44	8.82	8.14	6.90	2.55	2.64	2.87
Tm	0.41	0.33	0.32	0.15	0.34	0.35	1.28	1.10	1.01	0.36	0.38	0.42
Yb	2.56	2.14	2.00	0.93	2.08	2.15	8.07	6.12	5.97	2.17	2.31	2.55
Lu	0.40	0.35	0.32	0.13	0.33	0.33	1.26	0.92	0.82	0.34	0.36	0.41
Ba	397.65	1,326.61	1,128.86	1,361.26	1,326.16	309.86	1,919.71	2,281.61	40.13	683.90	880.18	1,327.91
Th	10.03	8.20	8.00	14.89	7.98	0.86	20.51	14.07	11.50	3.14	4.52	6.14
Nb	10.07	30.52	24.36	19.13	31.06	4.97	21.56	21.91	16.38	24.08	34.42	40.46
Y	28.52	22.74	21.65	12.81	22.73	21.68	79.41	74.60	72.93	23.85	24.67	27.05
Hf	4.45	4.33	4.15	6.82	4.27	1.94	15.02	12.90	1.92	3.18	3.69	3.88
Ta	0.69	1.96	1.58	0.99	1.99	0.34	1.44	0.94	1.60	1.41	2.08	2.35
U	1.65	1.81	1.70	2.10	1.88	0.23	2.09	0.96	2.28	0.77	1.13	1.47
Pb	15.86	13.90	13.88	16.72	17.71	2.92	30.57	22.09	52.45	10.18	7.84	8.42
Rb	56.43	54.19	52.00	88.71	48.03	64.06	113.89	79.36	36.70	26.36	39.56	50.25
Cs	3.14	0.91	1.00	1.00	0.82	0.26	0.24	0.16	0.25	0.29	1.02	0.75
Sr	172.27	505.08	404.22	692.04	526.20	181.72	105.23	137.05	28.18	479.70	512.48	712.27
Sc	9.94	17.56	17.20	9.59	17.98	45.70	7.87	15.14	2.17	25.24	25.75	19.87
Zr	167.59	174.34	169.72	294.91	172.78	68.04	591.90	507.93	20.51	130.62	151.74	162.22

Sample ID	VC-30	VC-32	VC-33	VC-34	VC-35*	VC-38	VC-39	VC-40*	VC-41	VC-42
Map unit	Tvcu	Tp	Yp	Aqfg	Tvcl	Yp	Yd	Tp	Aqfg	Aqfg
Lithology	Ba TAnd lava	Da porphyry	Pegmatite	Gneiss	Ba lava	Pegmatite	Diabase	Da porphyry	Gneiss	Gneiss
Latitude (°N)	45.2863	45.2931	45.2867	45.2867	45.2876	45.2815	45.3682	[illegible]	[illegible]	[illegible]
Longitude (°W)	111.8960	111.9517	111.9496	111.9497	111.9462	111.9707	111.9276	[illegible]	[illegible]	[illegible]
Major elements (wt%)										
SiO_2	50.99	60.11	73.74	73.03	50.78	73.68	51.69	[illegible]	[illegible]	[illegible]
TiO_2	1.32	0.47	0.05	0.46	1.05	0.01	2.47	[illegible]	[illegible]	[illegible]
Al_2O_3	16.11	14.50	13.99	11.89	14.65	14.12	12.90	[illegible]	[illegible]	[illegible]
FeO*	8.14	3.11	0.50	4.16	9.55	0.11	15.23	[illegible]	[illegible]	[illegible]
MnO	0.15	0.13	0.00	0.06	0.17	0.00	0.21	[illegible]	[illegible]	[illegible]
MgO	8.22	1.98	0.07	0.61	9.19	0.02	3.97	[illegible]	[illegible]	[illegible]
CaO	8.28	6.66	0.53	0.71	8.76	0.31	7.55	[illegible]	[illegible]	[illegible]
Na_2O	3.48	3.35	2.49	2.22	2.49	2.17	2.77	[illegible]	[illegible]	[illegible]
K_2O	2.02	2.79	7.54	5.48	1.44	8.60	1.46	[illegible]	[illegible]	[illegible]
P_2O_5	0.41	0.16	0.01	0.08	0.30	0.01	0.22	[illegible]	[illegible]	[illegible]
Sum	99.12	93.26	98.92	98.69	98.37	99.03	98.48	[illegible]	[illegible]	[illegible]
LOI	0.39	6.13	0.35	0.32	1.01	0.31	0.83	[illegible]	[illegible]	[illegible]
Trace elements (ppm)										
Ni+	144.77	18.10	5.67	6.90	238.20	3.90	40.18	[illegible]	[illegible]	[illegible]
Cr+	245.47	32.20	15.72	3.80	498.79	3.50	17.33	[illegible]	[illegible]	[illegible]
V+	158.80	62.40	3.48	14.90	196.21	3.60	448.19	[illegible]	[illegible]	[illegible]
Ga+	16.02	17.60	14.53	19.20	15.72	14.30	24.05	[illegible]	[illegible]	[illegible]
Cu+	23.48	8.80	1.39	40.40	63.88	0.60	212.93	[illegible]	[illegible]	[illegible]
Zn+	83.98	54.60	14.23	95.50	91.94	14.30	129.06	[illegible]	[illegible]	[illegible]
La	39.64	47.15	4.21	82.74	37.99	5.09	20.40	[illegible]	[illegible]	[illegible]
Ce	74.89	80.50	4.86	164.47	72.63	7.70	46.93	[illegible]	[illegible]	[illegible]
Pr	8.75	8.53	0.74	17.31	8.56	0.87	6.35	[illegible]	[illegible]	[illegible]
Nd	32.77	29.16	2.80	64.10	32.84	2.97	27.45	[illegible]	[illegible]	[illegible]
Sm	6.27	4.66	0.58	13.48	6.50	0.67	7.39	[illegible]	[illegible]	[illegible]
Eu	1.87	1.30	1.04	2.81	1.92	0.75	2.30	[illegible]	[illegible]	[illegible]
Gd	5.49	3.30	0.51	12.77	5.77	0.54	8.00	[illegible]	[illegible]	[illegible]
Tb	0.86	0.45	0.07	2.12	0.90	0.07	1.35	[illegible]	[illegible]	[illegible]
Dy	5.01	2.43	0.37	12.88	5.25	0.35	8.23	[illegible]	[illegible]	[illegible]
Ho	0.99	0.45	0.06	2.67	1.05	0.07	1.67	[illegible]	[illegible]	[illegible]
Er	2.68	1.13	0.16	7.29	2.79	0.16	4.38	[illegible]	[illegible]	[illegible]
Tm	0.38	0.15	0.02	1.05	0.39	0.02	0.61	[illegible]	[illegible]	[illegible]
Yb	2.34	0.93	0.11	6.24	2.45	0.12	3.70	[illegible]	[illegible]	[illegible]
Lu	0.36	0.13	0.02	1.00	0.37	0.02	0.55	[illegible]	[illegible]	[illegible]
Ba	1,263.87	1,662.04	2,425.71	1,959.06	986.67	1,679.43	254.12	[illegible]	[illegible]	[illegible]
Th	5.50	8.09	2.39	26.14	4.73	4.64	5.15	[illegible]	[illegible]	[illegible]
Nb	39.26	9.88	2.87	21.58	13.94	0.71	11.74	[illegible]	[illegible]	[illegible]
Y	25.12	12.74	1.65	67.66	26.48	1.68	40.61	[illegible]	[illegible]	[illegible]
Hf	3.97	3.85	0.22	16.30	4.76	0.46	5.61	[illegible]	[illegible]	[illegible]
Ta	2.31	0.58	0.31	0.91	0.70	0.08	0.85	[illegible]	[illegible]	[illegible]
U	1.51	1.98	0.09	2.47	0.87	0.25	1.37	[illegible]	[illegible]	[illegible]
Pb	14.28	23.78	36.58	41.50	6.68	45.28	7.28	[illegible]	[illegible]	[illegible]
Rb	47.38	52.02	170.40	145.60	33.81	190.61	57.25	[illegible]	[illegible]	[illegible]
Cs	0.83	0.80	0.55	0.73	0.86	0.46	1.18	[illegible]	[illegible]	[illegible]
Sr	655.97	655.82	149.52	61.84	583.77	104.41	184.92	[illegible]	[illegible]	[illegible]
Sc	23.60	6.25	0.67	4.84	26.39	0.23	32.42	[illegible]	[illegible]	[illegible]
Zr	166.48	144.53	7.19	635.67	194.51	13.76	204.70	[illegible]	[illegible]	[illegible]

Note. Lithology abbreviations: And, andesite; Ba, basalt; Da, dacite; TAnd, trachyandesite; TBa, trachybasalt.
All major elements and trace elements denoted by + were analyzed by XRF, all other trace elements were measured by ICP-MS.
FeO* indicates all Fe expressed as Fe^{2+}. LOI is loss on ignition. All samples were prepared and analyzed by X-ray fluorescence (XRF) and inductively coupled plasma mass spectrometry (ICP-MS) at the Washington State University GeoAnalytical Lab.
Datum used for sample coordinates is World Geodetic Survey 1984 (WGS84).
* Sample collected in landslide deposit.

TABLE 2. U-Pb GEOCHRONOLOGY.

Sample	Lithology	Unit	Latitude (°N)	Longitude (°W)	Mineral	# of Spot Analyses[a]	Age (Ma)	2σ	MSWD
VC-17	Tuff	Tvct	45.3501	111.9208	Zircon	11	34.0	0.3	1.1
VC-16	Andesite lava	Tvcu	45.3324	111.9535	Zircon	22	34.4	0.2	1.5
VC-37	Air-fall tuff	Tagt	45.3268	111.8782	Zircon	16	35.0	0.2	0.9
VC-08	Air-fall tuff	Tagt	45.2788	111.9305	Zircon	19	35.1	0.3	2.1
VC-36	Air-fall tuff	Tnct	45.3100	111.9720	Zircon	31	41.2	0.3	1.8
VC-40[b]	Dacite porphyry	Tp	45.3243	111.9682	Zircon	8	49.6	0.7	1.8
VC-06	Dacite porphyry	Tp	45.2868	111.9418	Zircon	21	49.9	0.3	1.3
VC-32	Dacite porphyry	Tp	45.2931	111.9517	Zircon	18	50.0	0.4	1.3
Pac6Pac1[c]	Hydrothermal mineralization	Aqfg	45.2498	111.9697	Xenotime	24	101.0	1.9	9.9

Note. Reported ages are the weighted mean of the ^{207}Pb corrected ^{206}Pb/^{238}U ages obtained for each sample. MSWD is the Mean Square Weighted Deviation. Zircon separates were prepared at MBMG and analyzed by LA-ICP-MS at the University of California, Santa Barbara. Latitudes and longitudes are in the 1984 World Geodetic Survey (WGS84) datum.
[a] Number of spot analyses used to calculate weighted mean age.
[b] Sample collected in landslide deposit.
[c] Sample collected at the pacific mine located in the adjacent Cirque Lake quadrangle, see text.

TABLE 3. ^{40}Ar/^{39}Ar GEOCHRONOLOGY.

Sample	Lithology	Unit	Latitude (°N)	Longitude (°W)	Material	%^{39}Ar	Age (Ma)	2σ	MSWD
VC-01	Ba lava	Tvcl	45.2807	111.9051	Groundmass	62.6	33.09	0.11	825
VC-13	Ba lava	Tvcm	45.3242	111.9473	Groundmass	48.3	32.99	0.12	2
VC-30	Ba TAnd lava	Tvcu	45.2863	111.8960	Groundmass	72.8	33.56	0.07	12

Note. Lithology abbreviations: Ba, basalt; TAnd, trachyandesite. Reported ages are the weighted mean plateau ages. Uncertainties are ± 2σ. MSWD is the Mean Square Weighted Deviation. Separates were prepared and analyzed at the New Mexico Institute of Mining and Technology.

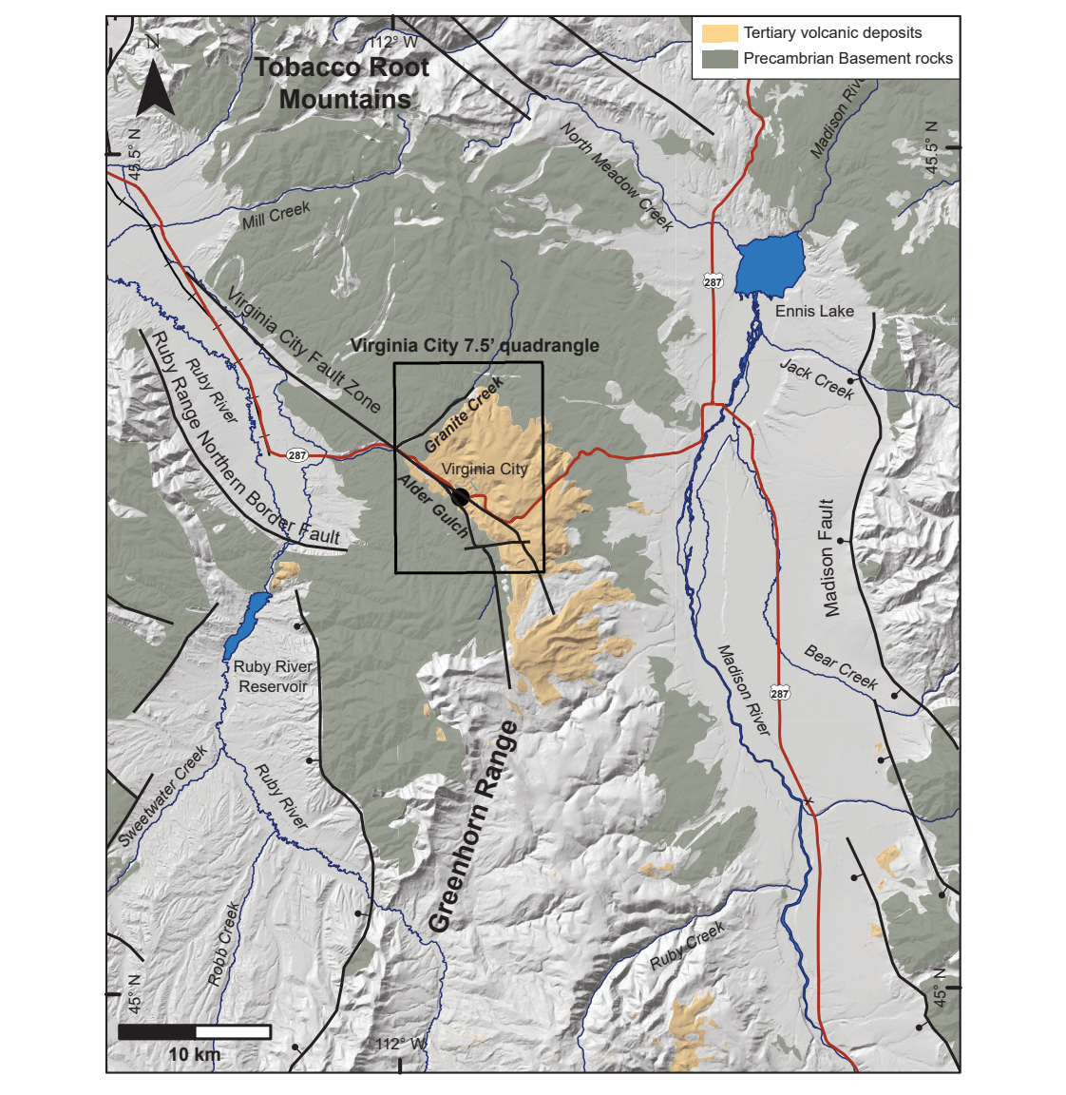

Figure 1. Simplified geologic map of the Virginia City area overlaid on a shaded digital elevation model (DEM). Geology modified from Ruppel and others (1993) and Kellogg and Williams (2006).

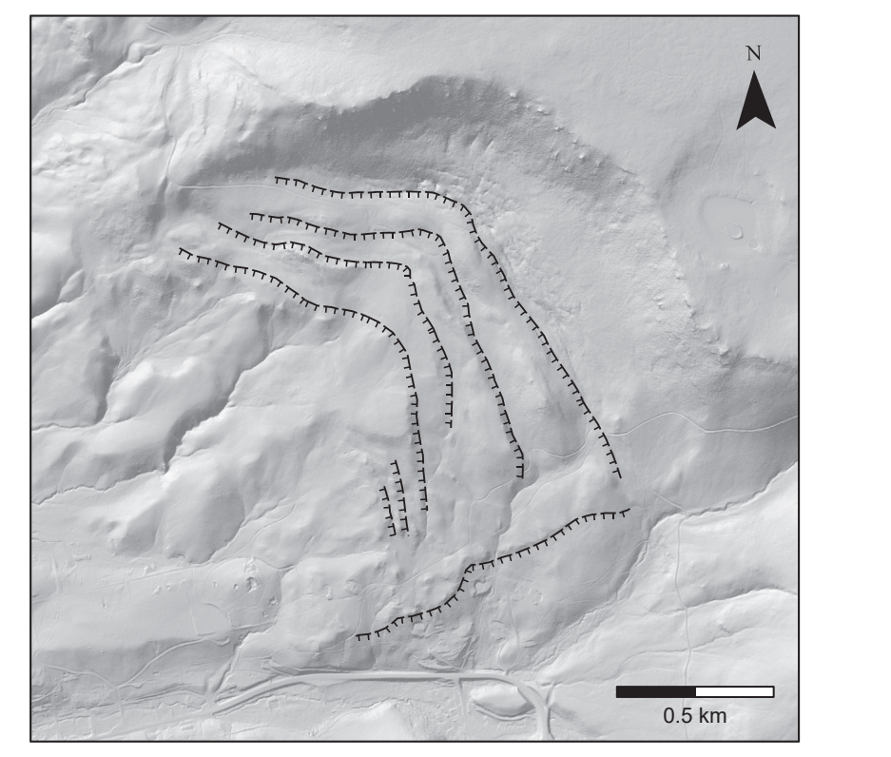

Figure 2. Landslide deposit formed in Cenozoic volcanic rocks (center of geologic map; where Qls intersects A–A' line). Lines with hachures show landslide scarps; hachures point down scarp. Image is a hillshade derived from LiDAR digital elevation model data collected as part of this study (Montana State Library, 2020).

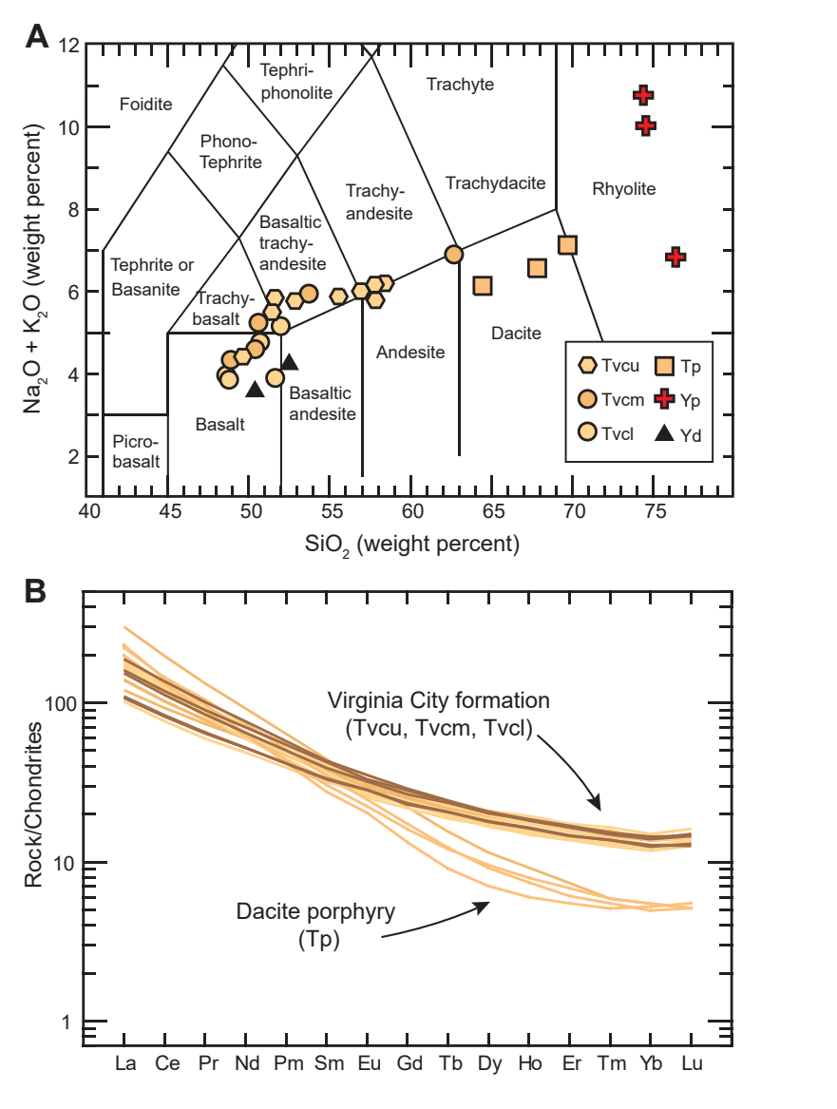

Figure 3. Whole rock geochemical data. (A) Total alkali silica classification diagram (after Le Bas and others, 1986). Values were normalized before plotting. (B) Chondrite-normalized rare earth element plot (after Sun and McDonough, 1989) of dacite porphyry (Tp) and the Virginia City Formation (Tvcu, Tvcm, and Tvcl). The plot traces are color-coded to match the legend in (A).

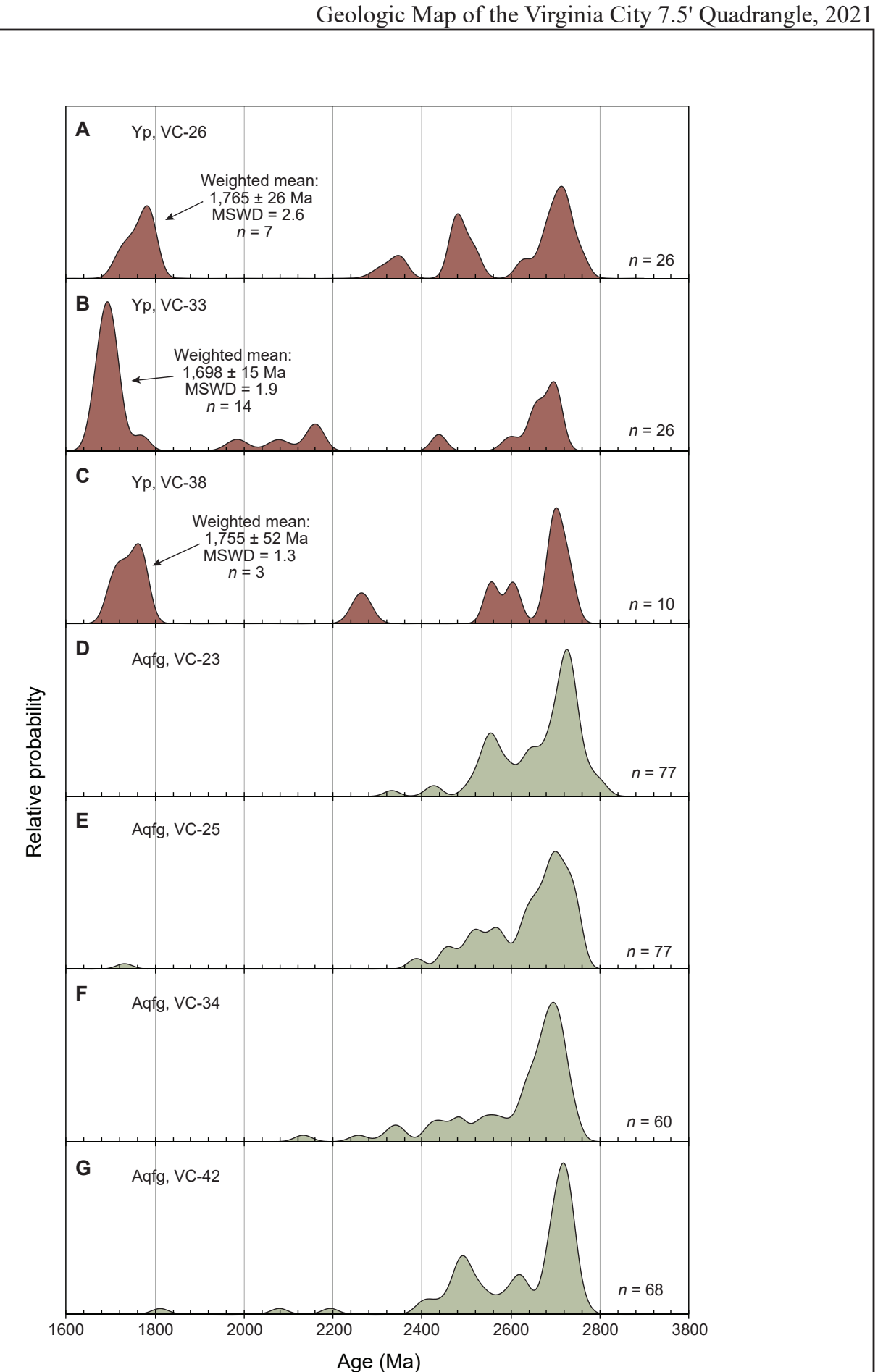

Figure 4. Probability density plots of ^{207}Pb/^{206}Pb zircon ages from Proterozoic pegmatite and Archean basement rocks. (A–C) Proterozoic pegmatite samples (VC-26, VC-33, and VC-38). All samples exhibit significant inheritance. The emplacement age is labeled on each plot. (D–G) Archean gneiss samples (VC-23, VC-25, VC-34, and VC-42).

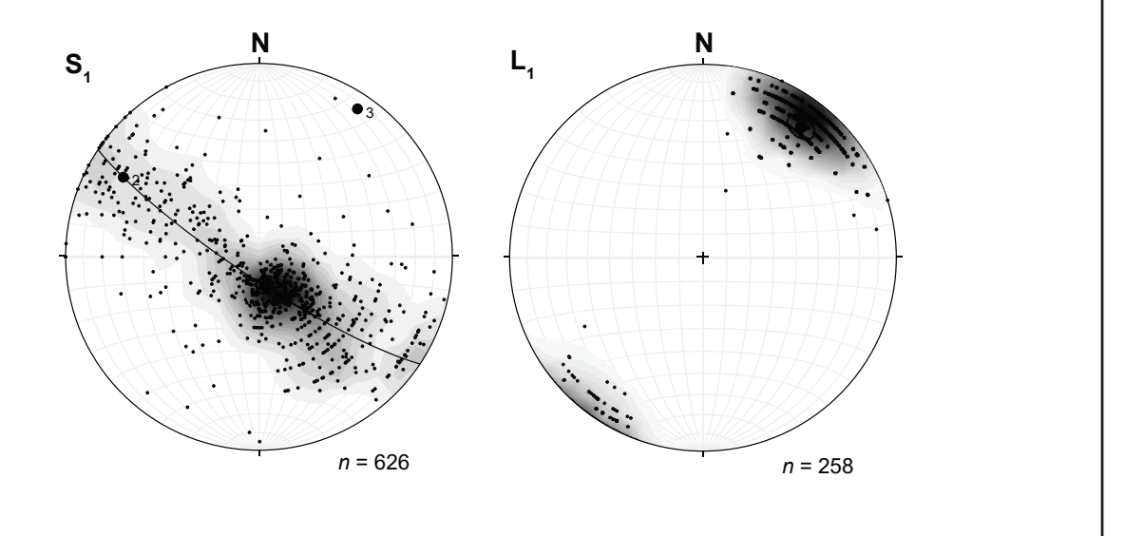

Figure 5. Lower-hemisphere projection of poles to the penetrative foliation (S_1) and lineations (L_1) measured in the Precambrian metamorphic rocks. Data are plotted on an equal-area stereonet and fit with a Kamb contour.

PHYSIOGRAPHIC SETTING AND HISTORICAL CONTEXT

The Virginia City 7.5' quadrangle is in Madison County Montana (fig. 1), spanning a low mountain pass separating the Tobacco Root Mountains from the Greenhorn Range. Elevations in the map area range from 1,649 to 2,275 m (5,410 to 7,464 ft) with an absolute relief of 626 m (2,054 ft). A plateau northeast of Virginia City covered by mixed timber and grassland is the highest and most prominent physiographic feature in the quadrangle. The lowest point in the map occurs along Alder Gulch, which is a major tributary to the Ruby River. Exposure of the bedrock geology is generally fair except where obscured by landslides shed from the high-standing volcanic tablelands.

Virginia City is one of Montana's oldest and most famed mining districts. The town was founded soon after placer gravels were discovered in Alder Gulch circa 1863, and eventually replaced Bannack as the territorial capital of Montana. The gravels in Alder Gulch proved to be one of the world's richest known placer concentrations, ultimately producing more than 2,500,000 oz of gold and about 350,000 oz of silver (Shawe and Wier, 1989). Some lode mines were operating at the time of this report, but the Virginia City mining district has never regained the activity of the late 1800s.

GEOLOGIC SUMMARY

The oldest rock in the map area is Archean gneiss interlayered with subordinate amphibolite, marble, quartzite, and isolated bodies of ultramafic rock (Aqfg, Au, and Am). This metamorphic assemblage provides a record of temporally distinct tectonothermal events ca. ~2.7 Ga, ~2.5–2.4 Ga, and ~1.8 Ga. Numerous Proterozoic pegmatite (Yp) and diabase (Yd) intrusions crosscut the Archean rocks throughout the map area and appear to intrude northwest-, east–west-, and northeast-oriented fractures. The Precambrian basement rocks were deeply exhumed by Late Cretaceous–Tertiary crustal shortening, eroding much of the Phanerozoic sedimentary overburden. Late Eocene to early Oligocene (~41–33 Ma) volcanogenic rocks composing the Virginia City volcanic group (Tvcu, Tvct, Tvcm, Tvcl, Tagt, and Tnct) rest on a nonconformity cutting the exhumed Precambrian rocks. These volcanic sequences generally consist of mafic-to-intermediate lavas intercalated with subordinate rhyolitic tuff intervals and minor gravel deposits. Scattered outcrops of dacite porphyry (Tp; ~50 Ma), most of which are surrounded by landslide deposits, represent an older volcanic system unrelated to the younger bi-modal volcanism recorded by the Virginia City group. A northwest-trending, left-lateral fault system (Virginia City Fault Zone; see Ruppel and Liu, 2004) transects the quadrangle and deforms Archean metamorphic rocks and Cenozoic volcanic units. Large mass wasting deposits occur throughout the map area, most of which are formed in the Cenozoic volcanic units. Quaternary gravels that were historically mined for placer gold and silver occur in extensive dredge tailings throughout the Alder Gulch stream drainage.

PREVIOUS MAPPING

Parts of the Virginia City 7.5' quadrangle were previously mapped by Cordua (1973, scale 1:24,000), Wier (1982, scale 1:12,000), and Kellogg and Williams (2006; scale 1:100,000). Unit descriptions for the Archean rocks are adapted from Cordua (1973), Wier (1982), and Ruppel and Liu (2004).

METHODS

Field mapping

Geologic field mapping was conducted in the Virginia City 7.5' quadrangle in 2017 (~3.5 mo) as part of the United States Geological Survey STATEMAP program. The quadrangle was chosen to assist a groundwater investigation by the Montana Bureau of Mines and Geology, and to investigate the previously undocumented style and tempo of Cenozoic volcanism. A 1:24,000-scale topographic base, high-resolution satellite imagery, and Light Detection and Ranging (LiDAR) elevation data (fig. 2; Montana State Library, 2020) were utilized for field mapping. Structure and observational data were located using a handheld GPS device; structure data were measured with a traditional hand transit or electronic mobile device. Additional metamorphic foliation and lineation measurements were compiled from Cordua (1973) and Wier (1982). Field data were digitized to a geodatabase template published by the National Cooperative Geologic Mapping Program.

Major and trace element chemistry, U-Pb geochronology, and ^{40}Ar/^{39}Ar geochronology

Rock specimens selected for geochemistry and geochronology studies were crushed at the MBMG mineral separation laboratory. A ~100–200 g split of the crushed material was prepared and analyzed by X-ray fluorescence (XRF) and inductively coupled plasma mass spectrometry (ICP-MS) at the Peter Hooper GeoAnalytical Lab, Washington State University, Pullman. Zircon crystals were isolated from specimens chosen for U-Pb zircon dating using standard density and magnetic separation techniques at the MBMG mineral separation laboratory and subsequently analyzed by Laser Ablation ICP-MS at the University of California, Santa Barbara. Samples selected for ^{40}Ar/^{39}Ar geochronology were processed and analyzed by ICP-MS at the New Mexico Geochronology Research Laboratory.

Whole-rock chemical data are presented in table 1, figure 3, and appendix A. All LA-ICP-MS data are provided in appendix B. The weighted mean of the ^{207}Pb corrected ^{206}Pb/^{238}U zircon ages from igneous rocks and hydrothermal xenotime are provided in table 2; ^{207}Pb/^{206}Pb age distributions for metamorphic rocks and pegmatite dikes are shown in figure 4. ^{40}Ar/^{39}Ar ages are provided in table 3, and a complete summary of the associated analytical results are provided in appendix C. Descriptions of laboratory methods accompany each appendix. All data appendices are available with this map for download from the MBMG website.

DESCRIPTION OF MAP UNITS

The geologic map of the Virginia City 7.5' quadrangle shows rock units exposed at the surface or overlain by a thin surficial cover of soil and colluvium. Surficial sedimentary and mass wasting deposits are shown where they are thick and mappable at 1:24,000 scale. Igneous and metamorphic rocks are classified using the International Union of Geological Sciences nomenclature (Le Bas and Streckeisen, 1991; Schmid and others, 2007). Minerals in igneous and metamorphic rock units are listed in order of decreasing abundance. The Cenozoic volcanic stratigraphy was constructed utilizing field observations, petrography, geochemistry, and geochronology data collected in this study; volcanic units were named after local geographic features. Grain-size classification of unconsolidated and consolidated sediment is based on the Wentworth scale (Lane, 1947). Multiple lithologies within a rock unit are listed in order of decreasing abundance.

ANTHROPOGENIC DEPOSITS

md **Mining dumps (Quaternary: Holocene)**—Artificial fill composed of excavated, transported, processed, and emplaced rock and gravel. Consists mainly of dredged placer workings and dumps from lode mines. Most extensive in Alder Gulch. Thickness generally greater than 5 m (16 ft).

ALLUVIAL DEPOSITS

Qal **Alluvium (Quaternary: Holocene)**—Poorly sorted and stratified gravel, sand, silt, and clay along streams and their tributaries. Clasts are rounded to subrounded cobbles and smaller, with occasional boulders. Thickness greater than 5 m (16 ft).

Qac **Alluvium and colluvium (Quaternary: Holocene)**—Gravel, sand, and silt deposited by sheetwash alluvium and incorporated with locally derived colluvium. Occurs in ephemeral stream drainages formed in landslide deposits. Thickness less than 6 m (20 ft).

Qgr **Gravel deposits (Quaternary: Pleistocene?)**—Poorly sorted and stratified gravel, sand, silt, and clay. Clasts are generally cobble size and smaller with occasional boulders, and are rounded to subrounded. Thickness greater than 5 m (16 ft).

MASS WASTING DEPOSITS

The Tertiary volcanic rocks are prone to mass wasting and consequentially, numerous landslides and debris flow deposits rim the high-standing volcanic tablelands. Many of the landslides appear to fail within devitrified tuff intervals (e.g., Tagt) that are saturated with groundwater and emanate spring creeks locally. Relatively young landslide deposits (Qls) are easily identified in the field and in LiDAR digital elevation models, whereas the older dissected and eroded landslide deposits (Qlso) are harder to recognize. The most notable landslide complex in the map area is over 1.5 km (0.6 mi) wide and underlies the hummocky terrain northeast of the Virginia City town center (fig. 2).

Qls **Landslide deposit (Quaternary: Holocene)**—Slumps, slides, and debris flows that range from chaotically oriented debris to intact blocks of bedrock. Deposits commonly exhibit recognizable landforms associated with landslides including crowns, scarps, fissures, slump blocks, and toes.

Qlso **Older landslide deposit (Quaternary: Pleistocene?)**—Heavily eroded and dissected slumps, slides, and debris flow deposits. Although some of the older deposits are characterized by hummocks, primary landslide features are difficult to recognize in the field.

VIRGINIA CITY VOLCANIC GROUP

Dacite porphyry (Tp; ~50 Ma) was the oldest Cenozoic unit identified in the map area. Poor exposure and ambiguous field relationships confound whether this unit represents a series of lava flows (e.g., Marvin and others, 1974), a large subvolcanic intrusion, or a swarm of smaller intrusions. The Nevada City tuff (Tnct) was the oldest ash deposit identified and yielded a radiometric age of ~41 Ma, which is notably discordant with the other volcanic units. The tuff is covered by mass wasting deposits that further obscure its chronostratigraphic position in the volcanic sequence. The Alder Gulch tuff (Tgat) marks the chronostratigraphic base of the main Tertiary volcanic pile in the southeastern part of the quadrangle and is overlain by a ~200-m thick (655 ft) sequence of mafic to intermediate lavas intercalated with subordinate tuff and gravel deposits, herein named the Virginia City formation (Tvcu, Tvct, Tvcm, and Tvcl). These volcanic intervals generally record the eruption (circa ~35–34 Ma) of high-K, calc-alkaline melts enriched with incompatible elements (fig. 3; tables 1, 2). Many of the U-Pb and ^{40}Ar/^{39}Ar ages obtained for this sequence are not in stratigraphic order, perhaps indicative of zircon's long residence time in parental melts, or disturbance to the K-Ar isotope systematics of mafic lavas (e.g., excess Ar).

Virginia City formation (Tertiary: late Eocene–early Oligocene)—A ~200-m thick (655 ft) sequence of mafic to intermediate lava flows intercalated with minor tuff intervals and rare gravel deposits. Mapped as four separate members: upper (Tvcu), middle (Tvcm), lower (Tvcl), and interbedded tuff (Tvct).

Tvcu **Virginia City formation, upper member (Tvcu)**—Blocky, gray to maroon weathering, mafic-to-intermediate lavas (48.3–57.6 wt. percent SiO_2) that commonly form resistant ledges supporting the high tablelands in the quadrangle. Lavas are aphanitic, seriate, or porphyritic, and contain distinct quartz xenocrysts (<1 percent; <2 mm) and phenocrysts of olivine (up to 20 percent; <2 mm) and plagioclase (<2 percent; 1–2 mm) in a groundmass of flow-aligned plagioclase, olivine, and iron oxide microlites. Some flows are vesiculated. A sample collected in the upper reaches of Herman Gulch yielded a U-Pb zircon age of 34.4 ± 0.2 Ma (VC-16). Another sample collected above Highway 287 northeast of Daylight Creek yielded a ^{40}Ar/^{39}Ar age of 33.56 ± 0.07 Ma (VC-30). Thickness as much as 110 m (360 ft).

Tvct **Virginia City formation, tuff member (Tvct)**—Recessive, pale gray to white weathering, porphyritic tuff containing phenocrysts of broken potassium feldspar (<3 percent; <1 mm), quartz (<1 percent; <1 mm), and biotite (<1 percent; ~1 mm) in a groundmass of devitrified glass shards. Thickness as much as 12 m (40 ft). A sample collected south of Granite Creek in the northern part of the map yielded a U-Pb zircon age of 34.0 ± 0.3 Ma (VC-17).

Tvcm **Virginia City formation, middle member (Tvcm)**—Mafic to intermediate lavas (47.5–61.1 wt. percent SiO_2) that are typically maroon to gray weathering. Lava flows are aphanitic to slightly porphyritic, containing phenocrysts of olivine (3–5 percent; up to 2 mm), occasional plagioclase (3–5 percent; up to 4 mm), and rare quartz xenocrysts (<1 percent; up to 2 mm) in a matrix of plagioclase, olivine, and Fe-oxide microlites. Lavas are commonly vesiculated and contain quartz amygdales. A conspicuous, maroon weathering volcanic breccia with calcite cement as much as 15 m thick (50 ft) marks the base of Tvcm locally. A sample collected east of Herman Gulch yielded a ^{40}Ar/^{39}Ar age of 32.99 ± 0.12 Ma (VC-13). Thickness is as much as 120 m (400 ft).

Tvcl **Virginia City formation, lower member (Tvcl)**—Gray to black mafic lava flows (46.9–50.2 wt. percent SiO_2) that typically form recessive slopes beneath Tvcm. Individual flows have massive, coherent interiors separated by autobrecciated zones of scoria. Flow interiors exhibit well-developed flow banding and are vesiculated with quartz amygdales locally. Columnar jointing is common. Lavas are aphanitic to slightly porphyritic, containing phenocrysts of olivine (~5 percent; up to 2 mm) and occasional pyroxene (<2 percent; ~0.5 mm) in a groundmass of flow-aligned plagioclase microlites. A sample collected along Highway 287 in the Daylight Creek drainage yielded a ^{40}Ar/^{39}Ar age of 33.09 ± 0.11 Ma (VC-01). Marvin and others (1974) reported a K-Ar age of 34.4 ± 3.0 Ma for this unit. Thickness as much as 85 m (280 ft).

Tagt **Alder Gulch tuff (Tertiary: Eocene)**—Rhyolitic air-fall tuff, tuffaceous sandstone, and sparse gravel lenses. Tuffaceous intervals are pale gray to white and are typically devitrified to clay. Poorly exposed and commonly displaced in landslide deposits. This unit yielded U-Pb zircon ages of 35.1 ± 0.3 Ma (VC-08) and 35.0 ± 0.2 Ma (VC-37). Thickness as much as 85 m (280 ft).

Tnct **Nevada City tuff (Tertiary: Eocene)**—Poorly exposed, white to pale yellow weathering, fine-grained, air-fall tuff exposed along Highway 287 near Nevada City. Appears to be overlain or displaced by a landslide. This unit yielded a U-Pb zircon age of 41.2 ± 0.3 Ma (VC-36). Thickness unknown.

Tp **Dacite porphyry (Tertiary: Eocene)**—Resistant, gray weathering dacite porphyry (65.1–68.2 wt. percent SiO_2) containing euhedral phenocrysts of plagioclase (~30–40 percent; up to 4 mm), sanidine (<5 percent; up to 2 mm), biotite (<3 percent; 1–2 mm), and hornblende (<3 percent; 1–3 mm). Commonly crops out in mass wasting deposits. Three samples (VC-06, VC-32, and VC-40) yielded U-Pb zircon ages spanning 50.0 ± 0.4 Ma to 49.6 ± 0.7 Ma. Marvin and others (1974) reported K-Ar ages of 51.1 ± 1.9 Ma and 49.3 ± 2.5 Ma for dacite porphyry from a rock quarry located in a landslide deposit near the Virginia City town center.

PALEOZOIC SEDIMENTARY ROCKS

An irregular and somewhat puzzling outcrop of Madison Group strata ~500 m wide (1,650 ft) rests on Archean crystal basement near the southern boundary of the quadrangle; the relatively small extent and poor exposure of this outcrop precluded the identification of the Mission Canyon or Lodgepole Formations. The nature of the contact between the Madison Group strata and underlying basement is obscured at this location, but is likely a low-angle fault or landslide contact.

Mm **Madison Group, undivided (Mississippian)**—Light to dark gray, massive- to thick-bedded limestone. Contains zones of evaporate-solution breccia and chert stringers. Forms resistant outcrops locally. Likely strata of the Mission Canyon Formation. Thickness unknown.

PRECAMBRIAN INTRUSIVE AND METAMORPHIC ROCKS

The oldest rocks in the map constitute a heterogeneous assemblage of Archean gneiss, amphibolite, marble, quartzite, and small bodies of ultramafic rock. The protolith of this rock assemblage is likely a large granitic body crosscut by mafic intrusions and intercalated with thin screens of metasedimentary rock. U-Pb zircon data acquired in this study (fig. 4) record an intrusive age of ~2.7 Ga or older, and subsequent tectonothermal events ca. ~2.5–2.4 Ga and ~1.8–1.7 Ga, referred to as the Tendoy and Big Sky orogenies, respectively (e.g., Harms and others, 2004; Jones, 2008; Cramer, 2015). The Archean assemblage is heterogeneous at the outcrop scale but homogenous at the 1:24,000 map scale, and therefore was mapped as one unit except for thick outcroppings of marble (Am) and ultramafic rocks (Au) that were mapped separately. See Wier (1982) and Cordua (1973) for detailed outcrop maps of the Archean assemblage.

Pegmatite intrusions cut the Archean crystalline rocks throughout the Virginia City quadrangle, forming concentrated dike swarms in the southwestern part of the map area. Pegmatite analyzed in this study exhibited significant zircon inheritance with maximum emplacement ages of ~1.7 Ga (fig. 4), supporting a Proterozoic age. Diabase dikes also intrude the Archean basement and crosscut the pegmatite intrusions locally. The mafic intrusions are assumed to be related to Proterozoic diabase (~1.4 Ga) occurrences in the Ruby Range (Wooden and others, 1978; James, 1990). Both the pegmatitic and diabasic intrusions appear to intrude brittle faults and fractures.

Yd **Diabase (Mesoproterozoic?)**—West–northwest-striking diabase dikes (49.4–51.7 wt. percent SiO_2) are ~2–70 m thick (3–230 ft) and have continuous lengths exceeding 6 km (3.8 mi). The dikes do not exhibit evidence of high-grade metamorphism and cut the foliation of Archean metamorphic rocks, commonly forming resistant spines. Diabase intrusions are dark to greenish gray when fresh, and weather to a rusty brown color. Fresh surfaces reveal a holocrystalline texture composed of equal proportions of interlocking phenocrysts (1–2 mm) of plagioclase and pyroxene with minor amounts of hornblende, biotite, magnetite, ilmenite, quartz, and orthoclase. Primary minerals are commonly altered to epidote, chlorite, and clay minerals. A similar intrusion in the Ruby Range yielded a whole-rock Rb-Sr age of ~1.4 Ga (James, 1990).

Yp **Pegmatite (Mesoproterozoic?)**—Pegmatite dikes (73.7–75.8 wt. percent SiO_2) are generally thin (< 2 m; ~6 ft), non-foliated, and exhibit a wide range of orientations, but most are west–northwest-, east–west-, or northeast-trending. Pegmatite dikes are coarse-grained (6 mm to 30 cm) and composed of quartz, potassium feldspar, albite, and accessory amounts of muscovite, biotite, magnetite, tourmaline, beryl, apatite, chalcopyrite, and malachite. Dike zonation from a quartz core to a feldspathic rim is common. Muscovite from a zoned pegmatite in the Ruby Range yielded a K-Ar age of 1.66 Ga and a Rb-Sr age of 1.65 Ga (Giletti, 1966). U-Pb dating of zircon in this study yielded max emplacement ages of ~1.7 Ga (fig. 4).

Au **Ultramafic rocks (Archean?)**—Irregular bodies of foliated ultramafic rock that are up to ~500 m (1,640 ft) wide in plan view. Ultramafic rocks are black to dark greenish gray and fine- to coarse-grained, consisting of orthopyroxene, olivine, enstatite, spinel, hornblende, and magnetite. Commonly altered to serpentine, talc, and garnet. Similar rocks occur in the Greenhorn Mountains and Ruby Range (Berg, 1979; Desmarais, 1981).

Aqfg **Quartzofeldspathic gneiss and amphibolite (Archean)**—Heterogenous assemblage of quartzofeldspathic gneiss and subordinate amphibolite that were mapped as one unit with an unknown thickness.

Gneiss generally forms rounded and deeply weathered outcrops that are various shades of gray and reddish brown. Gneiss is fine- to coarse-grained, massive to strongly foliated and is generally composed of interlayered granitic, tonalitic, and quartz–feldspar–biotite gneiss that may also include hornblende, and rarely plagioclase; the quartz–feldspar–biotite gneiss is most common. Biotite is either disseminated throughout the rock or aligned in layers; garnet is common in all types of gneiss. Migmatic layering and crosscutting veins are also common.

Amphibolite commonly occurs as brown to dark gray weathering layers and lenses parallel to the penetrative foliation that range from less than 1 m (3 ft) thick, to over 500 m (1,640 ft) thick; unusually thick amphibolite intervals are heterogeneous and contain thin layers of gneiss. Amphibolite is fine- to coarse-grained, massive to strongly foliated, and contains equal proportions of hornblende and plagioclase, with subordinate amounts of quartz and garnet. Some occurrences contain as much as 25 percent garnet and as much as 60 percent hornblende. Occurrences are typically altered to green shchist facies by retrograde metamorphism and contain abundant chlorite, epidote, and clay minerals. Amphibolites are extensively migmatized.

Am **Marble and quartzite (Archean?)**—White to light gray weathering marble composed mainly of calcite and dolomite. Marble is typically fine- to medium-grained, but coarse-grained locally with crystals up to ~2.5 cm (~1 in). Thin intervals of quartzite sometimes occur adjacent to marble outcrops. A prominent, northeast-striking layer of marble ~100 m thick (330 ft) occurs east of Granite Creek.

STRUCTURAL GEOLOGY

Precambrian deformation

Archean rocks in the Virginia City quadrangle exhibit a penetrative foliation (S_1; fig. 5) that is generally parallel to compositional and migmatic layering. The foliation is developed in all Archean metamorphic lithologies, except the ultramafic rocks (Au) which cross cut the foliation. The foliation is interpreted to be axial planar to sheath and recumbent isoclinal folds formed during an early deformation event (D_1). These folds were then refolded into a series of gently northeast-plunging antiforms and synforms during a subsequent deformational event (D_2); the most notable antiform in the map area is the broad, upright Mill Creek antiform that is cored by quartzofeldspathic gneiss (Cordua, 1973). A gently northeast–southwest-plunging lineation (L_1; fig. 5), commonly expressed as a mineral lineation, is observed in all the Archean metamorphic lithologies and is interpreted to parallel fold axes formed during D_2 deformation. Proterozoic dikes, which likely formed along brittle faults and fractures, cross cut D_1 and D_2 fabrics, indicating that early metamorphism and folding occurred prior to ~1.7–1.4 Ga. U-Pb zircon data from this study (fig. 4) suggest early deformation (D_1 and D_2) may have occurred circa ~2.5–2.4 Ga (Tendoy orogeny), or ~1.8–1.7 Ga (Big Sky orogeny).

Cordilleran fold-thrust belt deformation

Northerly trending folds and thrust faults deformed Archean–Mesozoic strata throughout much of the Greenhorn Range south of the Virginia City quadrangle (Lonn and others, 2000; Kellogg and Williams, 2006). These structures presumably formed in the broken foreland of the advancing Late Cretaceous Cordilleran fold-thrust belt. Much of the Phanerozoic cover in the Virginia City quadrangle was exhumed and eroded during contractional shortening, exposing the deep-seated Precambrian basement rocks. An isolated outcrop of the Madison Group resting on Archean basement in the southern part of the map represents the only prevolcanic sedimentary cover preserved in the Virginia City quadrangle. The contact between the Madison Group and Archean basement is obscured but could possibly be a low-angle fault representing a thrust klippe, or a Cenozoic extensional detachment (e.g., Neill and Harms, 2007).

Cenozoic transtensional deformation

A northwest-striking, high-angle fault system, termed the Virginia City Fault Zone (Ruppel and Liu, 2004), is inferred to underlie Alder Gulch. This fault system presumably formed during Proterozoic time and has been repeatedly reactivated throughout the Phanerozoic, including left-lateral strike-slip movement during the Cenozoic (Cordua, 1973; Vitaliano and Cordua, 1979; James, 1990; Ruppel and Liu, 2004). The Virginia City Fault Zone displaces Archean metamorphic rocks and Cenozoic volcanic units in the Virginia City quadrangle, and Tertiary sedimentary intervals and poorly consolidated surficial deposits outside the quadrangle (Vitaliano and Cordua, 1979; Ruppel and Liu, 2004). A prominent layer of marble (Am) east of Granite Creek is tentatively correlated to an outcrop of similar lithology south of Alder Creek, demonstrating ~1.7 km (1.1 mi) of minimum cumulative left-lateral slip across the Virginia City Fault Zone. Southward, the fault system splays into at least two faults that deform Cenozoic volcanic deposits and older Precambrian rocks. Northwest-, northeast-, and east–west-trending, high-angle faults mapped in the quadrangle are likely linked to the Virginia City Fault Zone.

MINERALIZATION

Mineral deposits are hosted by quartz veins formed in Archean basement rocks, most of which are northwest- or northeast-trending. Veins appear to be closely controlled by and emplaced along fractures and faults (Lockwood, 1990). Three general types of veins occur in the district (Shawe and Wier, 1989; Barnard, 1993): (1) gold-bearing quartz veins; (2) quartz veins containing gold and silver, and base metals including lead, zinc, and copper; and (3) quartz veins containing silver and base metals, and a relatively minor amount of gold. The Virginia City mining district appears to be zoned, with gold-rich deposits at the center of the district near the head of Alder Gulch and silver–lead deposits in the outer periphery of the district (Shawe and Wier, 1989).

The origin of metal-bearing veins in the Virginia City district is poorly understood and somewhat debated. Ruppel and Liu (2004) postulated that veins were formed during Proterozoic magmatism and the emplacement of the pegmatite dike swarm. Others argue that vein formation and mineralization was linked to a concealed Late Cretaceous satellite stock of the Tobacco Root or Boulder Batholiths (e.g., Cole, 1983; Shawe and Wier, 1989; Eimon, 1997). Alternatively, the quartz veins may have been emplaced and remobilized over several recurring tectonothermal events (e.g., Ruppel, 1985). In this study, an altered granite collected at the Pacific Mine located to the south of Virginia City in the adjacent Cirque Lake quadrangle yielded a U-Pb xenotime age of ~101 Ma (table 2). The xenotime was likely formed by a magmatic-hydrothermal event that drove vein emplacement and related mineralization (Gammons and others, 2019). Hammarstrom and others (2002) reported a ^{40}Ar/^{39}Ar age of 120.2 ± 0.7 Ma for sericite collected in the Kearsarge Mine in the Virginia City mining district; however, the isotope systematics were disturbed by excess argon and the somewhat anomalous age was difficult to reconcile within the local geologic framework. In light of the U-Pb xenotime age presented herein, sericite may have indeed formed during a Late Cretaceous magmatic-hydrothermal event. While magmatic rocks of a similar age to hydrothermal xenotime and sericite were not identified in the Virginia City region, a granitic intrusion in the nearby Pioneer Mountains yielded a U-Pb zircon age of 105.2 ± 0.5 Ma (McDonald, in prep.), revealing a previously unrecognized episode of Early Cretaceous magmatism in southwest Montana that may have been linked to local hydrothermal mineralization.

ACKNOWLEDGMENTS

Stuart Parker helped perform mineral separations at the MBMG Mineral Separation Laboratory, and Gary Wyss assisted the SEM-CL work at the Montana Technological University, Butte. Andrew Kylander-Clark graciously supported LA-ICP-MS analyses and data reduction at the University of California, Santa Barbara. Ashley and Arron Steiner directed bulk-rock geochemical analyses at the Peter Hooper Geoanalytical Laboratory, Washington State University, Pullman. Dr. Jake Ross oversaw the ^{40}Ar/^{39}Ar geochronology performed at the New Mexico Institute of Mining and Technology's Geochronology Research Laboratory. Jeremy Crowley and Andy Bobst arranged the acquisition and processing of LiDAR elevation data utilized for landslide mapping. Andy Bobst also provided useful insights and interpretations of the area's geology from a geohydrological standpoint, specifically the mass wasting deposits. Geophysical data collected by Mohamed Khalil (Khalil and others, 2018) and the Montana Technological University's summer field course taught by Marvin Speece were helpful for mapping the large landslide complexes in the quadrangle. Technical reviews of the map by Phyllis Hargrave, Susan Vuke, and Catherine McDonald significantly improved the quality and presentation of the geologic information. Much of the geologic mapping would not have been possible without access to private lands granted by landowners. The Virginia City city council was pivotal to coordinating access to private lands.

REFERENCES

Barnard, F., 1993, District scale zoning pattern, Virginia City, Montana, USA: 96th National Western Mining Conference of the Colorado Mining Association (Denver), reprint 93-29, 18 p.
Berg, R.B., 1979, Precambrian geology of the west part of the Greenhorn Range, Madison County, Montana: Montana Bureau of Mines and Geology Geologic Map 6, 16 p., 2 sheets, scale 1:28,160.
Cole, M.M., 1983, Nature, age, and genesis of quartz-sulfide-precious metal vein systems in the Virginia City Mining District, Madison County, Montana: Bozeman, Montana State University, M.S. thesis, 76 p.
Cordua, W.S., 1973, Precambrian geology of the southern Tobacco Root Mountains, Madison County, Montana: Bloomington, Indiana University, Ph.D. dissertation, 147 p.
Cramer, M., 2015, Proterozoic tectonometamorphic evolution of the Ruby Range, SW Montana, USA: Insights from phase equilibria modeling in situ monazite petrochronology: Missoula, University of Montana, M.S. thesis, 79 p.
Desmarais, N.R., 1981, Metamorphosed Precambrian ultramafic rocks in the Ruby Range, Montana: Precambrian Research, v. 16, p. 67–101.
Eimon, P.I., 1997, The economic geology of Montana's Virginia City Mining District: Society of Economic Geologists Newsletter, no. 28, 6 p.
Gammons, C., Mosolf, J., and Poulson, S.R., 2019, Precious metal mineralogy, S-isotopes, and new LA-ICP-MS date for the Easton and Pacific lode mines, Virginia City District, Montana, *in* Scarberry, K.C., and Barth, S., eds., 2019, Proceedings of the Montana Mining and Mineral Symposium 2018: Montana Bureau of Mines and Geology Special Publication 120, 144 p.
Giletti, B.J., 1966, Isotopic ages from southwestern Montana: Journal of Geophysical Research, v. 71, p. 4029–4036.
Hammarstrom, J.M., Van Gosen, B.S., Kunk, M.J., and Herring, J.R., 2002, Gold-bearing quartz veins in the Virginia City mining district, Madison County, Montana: Northwest Geology, v. 31, p. 12–43.
Harms, T.A., Brady, J.B., Burger, H.R., and Cheney, J.T., 2004, Advances in the geology of the Tobacco Root Mountains, Montana, and their implications for the history of the northern Wyoming Province, *in* Brady, J.B., Burger, H.R., Cheney, J.T., and Harms, T.A., eds., Precambrian geology of the Tobacco Root Mountains, Montana: Geological Society of America Special Paper 377, p. 227–243.
James, J.L., 1990, Precambrian geology and bedded iron deposits of the southwestern Ruby Range, Montana: U.S. Geological Survey Professional Paper 1495, 39 p.
Jones, C., 2008, U-Pb geochronology of monazite and zircon in Precambrian metamorphic rocks from the Ruby Range, SW Montana: Deciphering geological events that shaped the NW Wyoming Province: Kent, Ohio State University, M.S. thesis, 119 p.
Kellogg, K.S., and Williams, V.S., 2006, Geologic map of the Ennis 30' x 60' quadrangle, Madison and Gallatin Counties, Montana, and Park County, Wyoming: Montana Bureau of Mines and Geology Open-File Report 529, 27 p., 1 sheet, scale 1:100,000.
Khalil, M., Bobst, A., and Mosolf, J., 2018, Utilizing 2D electrical resistivity tomography and very low frequency electromagnetics to investigate the geohydrology of natural cold springs near Virginia City, southwest Montana: Pure and Applied Geophysics, v. 175, p. 3525–3538.
Lane, E.W., 1947, Report of the subcommittee on sediment terminology: Transactions of the American Geophysical Union, v. 28, no. 6, p. 936–938.
Le Bas, M.J., LeMaitre, R.W., Streckeisen, A., and Zanettin, B., 1986, A chemical classification of volcanic rocks based on the total alkali silica diagram: Journal of Petrology, v. 27, p. 745–750.
Le Bas, M.J., and Streckeisen, A.L., 1991, The IUGS systematics of igneous rocks: Journal of the Geological Society of London, v. 148, p. 825–833.
Lockwood, M.S., 1990, Controls on precious-metal mineralization, Easton-Pacific vein, Virginia City mining district, Madison County, Montana: Socorro, New Mexico Institute of Mining and Technology, M.S. thesis, 149 p.
Lonn, J.D., Skipp, B., Ruppel, E.T., Janecke, S.U., Perry, W.J., Jr., Sears, J.W., Bartholomew, M.J., Stickney, M.C., Fritz, W.J., Hurlow, H.A., and Thomas, R.C., 2000, Geologic map of the Lima 30' x 60' quadrangle, southwest Montana: Montana Bureau of Mines and Geology Open-File Report 408, 42 p., 2 sheets, scale 1:100,000.
Marvin, R.F., Wier, K.L., Mehnert, H.H., and Merritt, V.M., 1974, K-Ar ages of selected Tertiary igneous rocks in southwestern Montana: Isochron West, no. 10, p. 17–20.
McDonald, C., submitted to the USGS, June 2018, Geologic map of the Ermont 7.5' quadrangle, Beaverhead County, Montana: Montana Bureau of Mines and Geology Open-File Report, 1 sheet, scale 1:24,000.
Montana State Library, 2020, Montana Lidar inventory, available at https://geoinfo.msl.mt.gov/Home/msdi/elevation [Accessed June 2021].
Neill, O.K., and Harms, T.A., 2007, Absence of lower Paleozoic stratigraphic section as evidence for Tertiary extension in southwest Montana: Geological Society of America Abstracts with Programs, v. 39, no. 1, p. 74.
Ruppel, E.T., and Liu, Y., 2004, The gold mines of the Virginia City mining district, Madison County, Montana: Montana Bureau of Mines and Geology Bulletin 133, 83 p., 2 sheets.
Ruppel, E.T., 1985, The association of Middle Cambrian rocks and gold deposits in southwest Montana: U.S. Geological Survey Open-File Report 85-207, 26 p.
Ruppel, E.T., O'Neill, J.M., and Lopez, D.A., 1993, Geologic map of the Dillon 1º x 2º quadrangle, Idaho and Montana: U.S. Geological Survey Miscellaneous Investigations Series Map I-1803-H, scale 1:250,000.
Schmid, R., Fettes, D., Harte, B., Davis E., and Desmons, J. A., 2007, Systematic nomenclature for metamorphic rocks: 1. How to name a metamorphic rock: Recommendations by the IUGS Subcommission on the Systematics of Metamorphic Rocks, https://www.bgs.ac.uk [Accessed June 24th, 2019].
Shawe, D.R., and Wier, K.L., 1989, Gold deposits in the Virginia City-Alder Gulch district, Montana: U.S. Geological Survey Bulletin 1857-G, p. G14–G19.
Sun, S.S., and McDonough, W.F., 1989, Chemical and isotope systematics of oceanic basalts: Implications for mantle composition and processes, *in* Saunders, A.D. and Norry, M.J., eds., Magmatism in the ocean basins: Geological Society, London, Special Publications, v. 42, p. 313–345.
Wooden, J.L., Vitaliano, C.J., Koehler, S.W., and Ragland, P.C., 1978, The late Precambrian mafic dikes of the southern Tobacco Root Mountains, Montana: Canadian Journal of Earth Sciences, v. 15, p. 467–479.
Vitaliano, C.J., and Cordua, W.S., 1979, Geologic map of the southern Tobacco Root Mountains, Madison County, Montana: Geological Society of America Map and Chart Series MC31, 8 p., scale 1:62,500.
Wier, K.L., 1982, Map showing geology and outcrops of the Virginia City and Alder quadrangles, Madison County, Montana: U.S. Geological Survey Miscellaneous Field Studies Map MF-1490, scale 1:12,000.

MBMG
Montana Bureau of Mines and Geology

Geologic Map 80

Geologic Map of the Virginia City 7.5' Quadrangle, Madison County, Montana

Jesse G. Mosolf

2021